

NEW HORIZON IN BIOIMAGING AND BIOMAGNETICS

Shoogo Ueno and Masaki Sekino

Department of Biomedical Engineering, Graduate School of Medicine, The University of Tokyo,
Tokyo 113-0033, Japan

Emails: ueno@medes.m.u-tokyo.ac.jp

Abstract- This paper reviews the recently developed techniques in biomagnetics and bioimaging such as transcranial magnetic stimulation (TMS), magnetic resonance imaging (MRI), and cancer therapy based on magnetic stimulation. A technique of localized and vectorial TMS has enabled us to obtain non-invasive functional mapping of the human brain. The development of new bioimaging technologies such as current distribution MRI and conductivity MRI potentially enables us to understand the dynamics of brain functions, which include millisecond-level changes in functional regions and dynamic relations between brain neuronal networks. These techniques are leading medicine and biology into a new horizon through the novel applications of magnetism. A lecture on current limiter intended specifically for engineering students pursuing specialization with Electrical and Electronics engineering is proposed in this paper. The important information which doesn't appear in text books are presented to the students. A general overview of different techniques of limiting fault current in electric power systems with special emphasis on two types of current limiters based on passive magnetic materials and high temperature superconducting materials have been presented. Simple laboratory experiments are also proposed to validate the theoretical knowledge.

Index terms: Biomagnetics, bioimaging, transcranial magnetic stimulation, magnetic resonance imaging, brain Function

[1] INTRODUCTION

Biomagnetics is a new research field for scientific investigation of the relations between living organisms and magnetism [1]. Applying an interdisciplinary approach, it covers a wide range of fields from medicine and biology to physics and engineering. A technique of localized and vectorial transcranial magnetic stimulation (TMS) has enabled us to obtain non-invasive functional mapping of the human brain [2-4]. Recent studies have shown that TMS potentially has therapeutic effects for several diseases such as mental illnesses, ischemia, and cancer [5-15].

The development of bioimaging technologies such as functional magnetic resonance imaging (MRI) and magnetoencephalography (MEG) enabled the identification of the locations of human brain functions. Despite these technologies, however, it is still difficult to understand the dynamics of brain functions, which include millisecond-level changes in functional regions and dynamic relations between brain neuronal networks. We are developing a new imaging principle of MRI for visualizing neuronal electrical activities and electrical conductivities in the brain [16-23]. This method potentially has millisecond-order high temporal resolution and millimeter-order high spatial resolution. In this paper, recent advances in biomagnetics and bioimaging for studying brain functions are reviewed and discussed based on the results obtained mainly in our laboratory. The review includes TMS, MRI, and cancer therapy based on magnetic stimulation.

[2] TRANSCRANIAL MAGNETIC STIMULATION

Our devised method of localized brain stimulation uses a figure-eight coil [2,3]. When a strong electric current is applied to a figure-eight coil over the head for 0.1 ms, a pulsed magnetic field of 1 T is produced. This magnetic field generates eddy currents in the brain, which stimulate the neurons. For example, by electrically stimulating the motor area of the brain, which is responsible for movement control, a person's fingers can be induced to move involuntarily. We have succeeded in selectively stimulating the human cerebral cortex with a spatial resolution of 3-5 mm. TMS is a useful method to examine brain function and structure without causing any pain. In recent years, an increasing number of studies on the clinical applications of magnetic stimulation have been performed. There are high expectations for magnetic stimulation to regulate paralysed muscles, promote regeneration of a damaged nervous system, regulate gene expression, and compensate for the loss of sensory functions. TMS may also provide beneficial therapeutic applications in treating patients with pain and psychoneurotic disorders. Results obtained in recent studies concerning TMS have provided a basic understanding of its clinical application in the treatment of depression and Parkinson's disease, as well as its clinical usefulness in protecting or repairing neurons damaged by cerebral infarction or other brain injury.

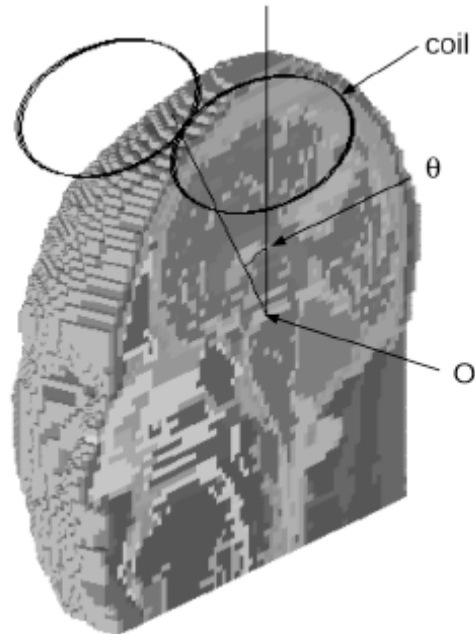


Fig. 1. Numerical Model Of Transcranial Magnetic Stimulation (TMS) With A 75-Mm Figure-Eight Coil [7].

TMS has been used for psychiatric treatment in numerous studies as an alternative to electroconvulsive therapy (ECT). However, the difference in current distributions between these therapies has not been clarified. Numerical simulations of ECT and TMS were carried out using a simplified three-layer model and a detailed model of the human head [5-7]. The simplified model was constructed from magnetic resonance images. The model consisted of 3 types of tissues with different conductivities representing the brain, the skull, and the scalp. In the ECT model, a voltage of 100 V was applied through electrodes which were located at unilateral and bilateral positions. In the TMS model, a figure-eight coil (6 cm diameter per coil) was placed on the vertex of the head model. An alternating current with a peak intensity of 3.0 kA and a frequency of 4.2 kHz was applied to the coil. Because the skull had a relatively low conductivity, a significant amount of the current flowed along the scalp and did not penetrate the skull. The maximum current density in the brain was 266 A m^{-2} in unilateral ECT, and 234 A m^{-2} in bilateral ECT. While the skull significantly affected current distributions in ECT, neither the skull nor the scalp disturbed the magnetic fields in TMS because the magnetic permeability of the tissues was almost equal to that of air. Thus, the magnetic fields efficiently induced eddy currents in the brain.

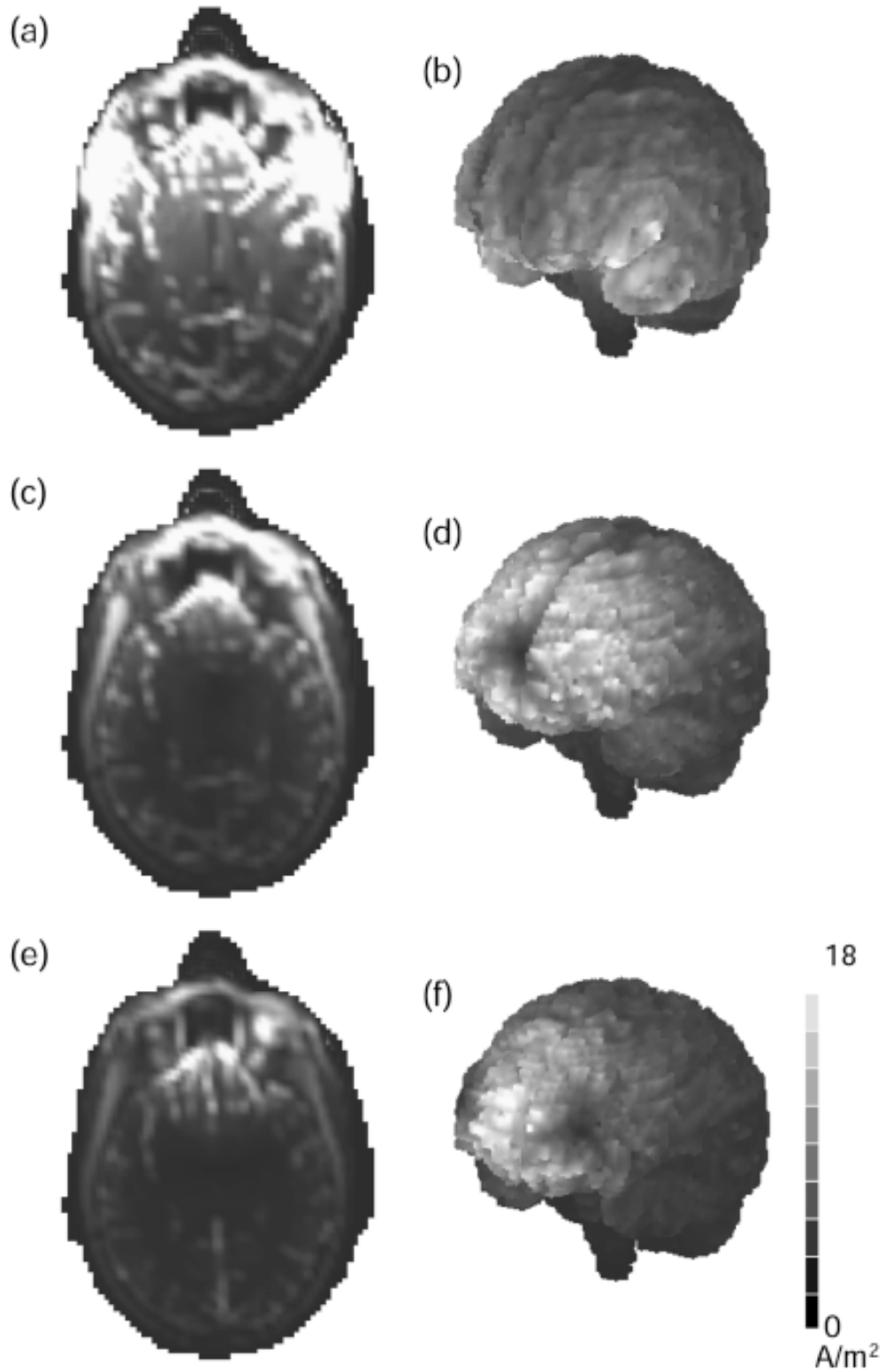


Fig. 2. (A)(B) Current Distributions In ECT. (C)(D) Current Distributions In TMS By A 100-Mm Circular Coil. (E)(F) Current Distributions In TMS By A 75-Mm Figure-Eight Coil [7].

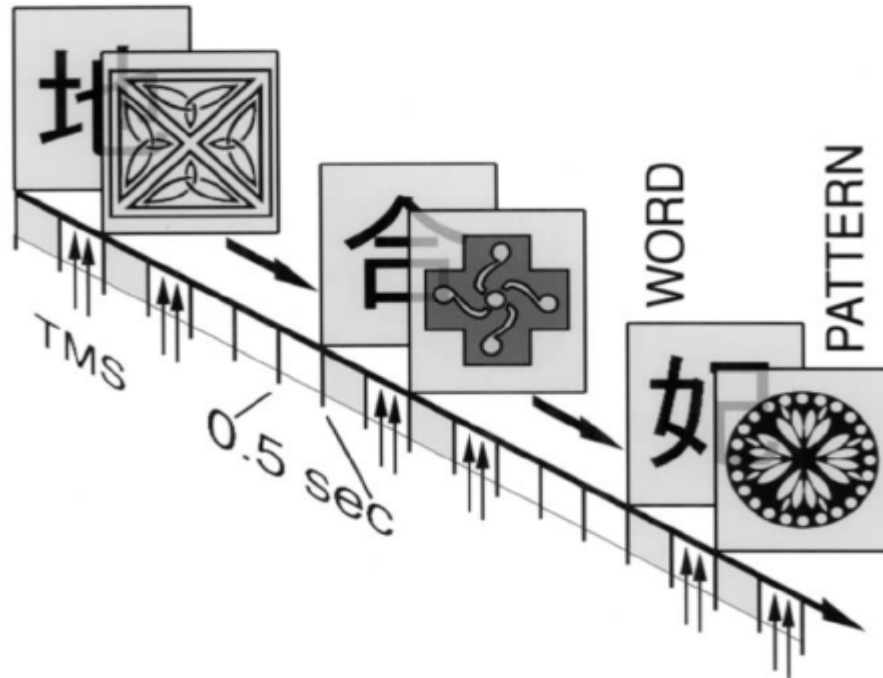


Fig. 3. Timeline (Left To Right) For Presentation Of Kanji Words And Abstract Patterns In One Trial Of 9s Duration. Pulses Of TMS Are Indicated By Paired Vertical Arrows. Shaded Areas Beneath The Baseline Indicate When Cognitive Stimuli Are Visible [4].

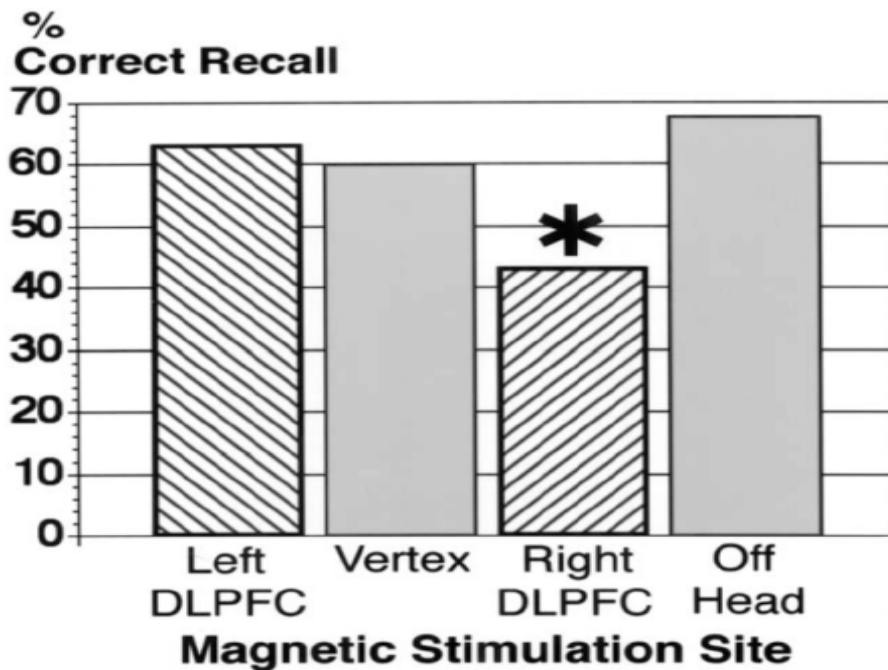


Fig. 4. Overall Percent Correct For Subsequent Recall Of Paired Associates According To Site Of TMS. The Comparison Of Interest Is Between The Left And Right DLPFC, With An Active TMS Control At The Vertex. In A Second Control, The Magnetic Coil Is Off The Head. The Asterisk Indicates $P < 0.05$ For Right Vs. Left DLPFC [4].

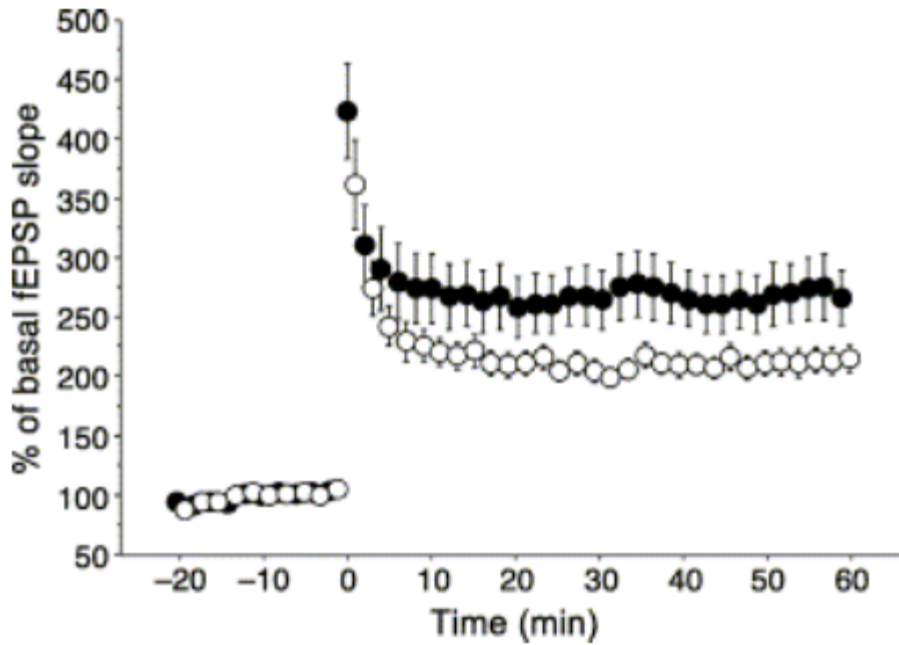


Fig. 5. Ltps Of 0.75 T Stimulated And Sham Control Groups. The Maintenance Phase Of The LTP Of The Stimulated Group (Black Circle) Was Significantly Enhanced Compared With The Sham Control Group (White Circle) ($P = 0.0408$) [8].

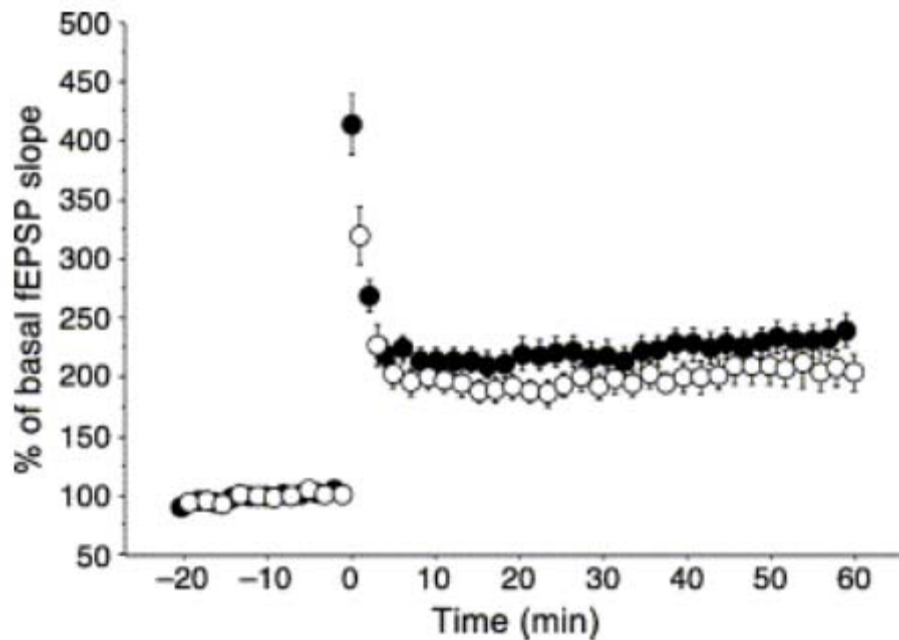


Fig. 6. Ltps Of 1.00 T Stimulated And Sham Control Groups. There Was No Significant Difference ($P = 0.1948$) Between The Maintenance Phase Of The LTP Of The Stimulated Group (Black Circle) And The Sham Control Group (White Circle) [8].

The maximum current density of 322 A m^{-2} was found under the intersection of the coil on the scalp, which was comparable to the maximum current density in ECT. TMS exhibited much lower current densities in the scalp in comparison with ECT. In another study, the optimum conditions of TMS as an alternative to ECT were determined using a detailed model. The model had a spatial resolution of 4 mm and 24 tissues with different conductivities. Electrodes in the ECT model were located at the bilateral position. In the TMS model, eddy current distributions were obtained for figure-eight coils with diameters of 50 mm, 75 mm, and 100 mm, and coil positions varied from the vertex to the forehead. A performance function was defined to evaluate the difference in current distributions in ECT and TMS. The optimum conditions of TMS were determined by finding a minimum value of the function. The function decreased with an increase in the coil diameter. This was because eddy currents induced by larger coils distributed in larger and deeper areas. The function decreased with the coil position approaching to the forehead. The coil of 100-mm diameter gave the minimum value of the function ($53 \text{ A}^2 \text{ m}^{-4}$) at a coil current of 87 kA, which corresponded to a magnetic flux density of 1.1 T. This study clarified difference in current distributions between ECT and TMS. In addition, the optimal condition of TMS for psychiatric disease was determined.

TMS is a useful method to examine dynamic brain function without causing any pain, producing so-called “virtual lesions” for a short period of time. We were able to non-invasively evaluate the cortical reactivity and functional connections between different brain areas. We studied an associative memory task involving pairs of Kanji (Chinese) pictographs and unfamiliar abstract patterns [4]. Subjects were ten Japanese adults fluent in Kanji, so only the abstract patterns represented novel material. During memory encoding, TMS was applied over the left and right dorsolateral prefrontal cortex (DLPFC). A significant ($P < 0.05$) reduction in subsequent recall of new associations was seen only with TMS over the right DLPFC. This result suggests that the right DLPFC contributes to encoding of visual-object associations.

Recently, repetitive TMS (rTMS) has become an increasingly important therapeutic tool for the potential treatment of neurological and psychiatric disorders. We investigated the effect of rTMS on long-term potentiation (LTP) in the rat hippocampus [8]. Rats were magnetically stimulated at

a rate of 1000 pulses/day for 7 days by a circular coil, in which the peak magnetic fields at the center of the coil were 0.75 and 1.00 T. LTP enhancement was observed only in the 0.75-T rTMS group, while no change was observed in the 1.00-T rTMS group. These results suggest that the effect of rTMS on LTP depends on the stimulus intensity. In another study, LTP was induced after the hippocampal slices were exposed to ischemic conditions [9]. The LTP of the stimulated group was enhanced compared with the LTP of the sham control group in each ischemic condition, suggesting that rTMS resulted in acquisition of ischemic tolerance in the hippocampus.

The effect of rTMS on injured neurons was investigated in the rat brain after administration of the neurotoxin MPTP (1-methyl-4-phenyl-1,2,3,6-tetrahydropyridine) [10]. The rats received rTMS (10 trains of 25 pulses/s for 8 s) 48 h after MPTP injection. Tyrosine hydroxylase (TH) and NeuN expressions were investigated in the substantia nigra. The functional observational battery hunched posture score for the MPTP-rTMS group was significantly lower and the number of rearing events was higher compared with the MPTP-sham group. These results suggest that rTMS reactivates the dopaminergic system in the brain.

[3] MAGNETIC RESONANCE IMAGING

Estimation of conductivity distributions in the brain is essential for various analyses in biomedical engineering, such as obtaining current distributions in electric stimulation and magnetic stimulation, calculating the absorption of electromagnetic waves from mobile phones, and current source estimations in electroencephalography and magnetoencephalography. We obtained conductivity distributions in the rat brain and the human brain using MRI [16,17]. Our method was based on the proportionality between the self-diffusion coefficient of water and conductivity. Images of the rat brain were obtained using a 4.7 T MRI system, with the stimulated echo acquisition mode (STEAM) sequence and a spinecho imaging sequence. Five animals were used in each measurement. Motion probing gradients (MPGs) were applied in 6 directions. Numbers of b factor steps in the STEAM and spin-echo measurements were 61 and 4, respectively. The diffusion coefficient and the fractional volume of extracellular space were estimated from the relationship between the signal intensity and the b factor. The estimation was

based on the model that the fast component of diffusion originated from the extracellular space. The effective conductivity of tissues was estimated.

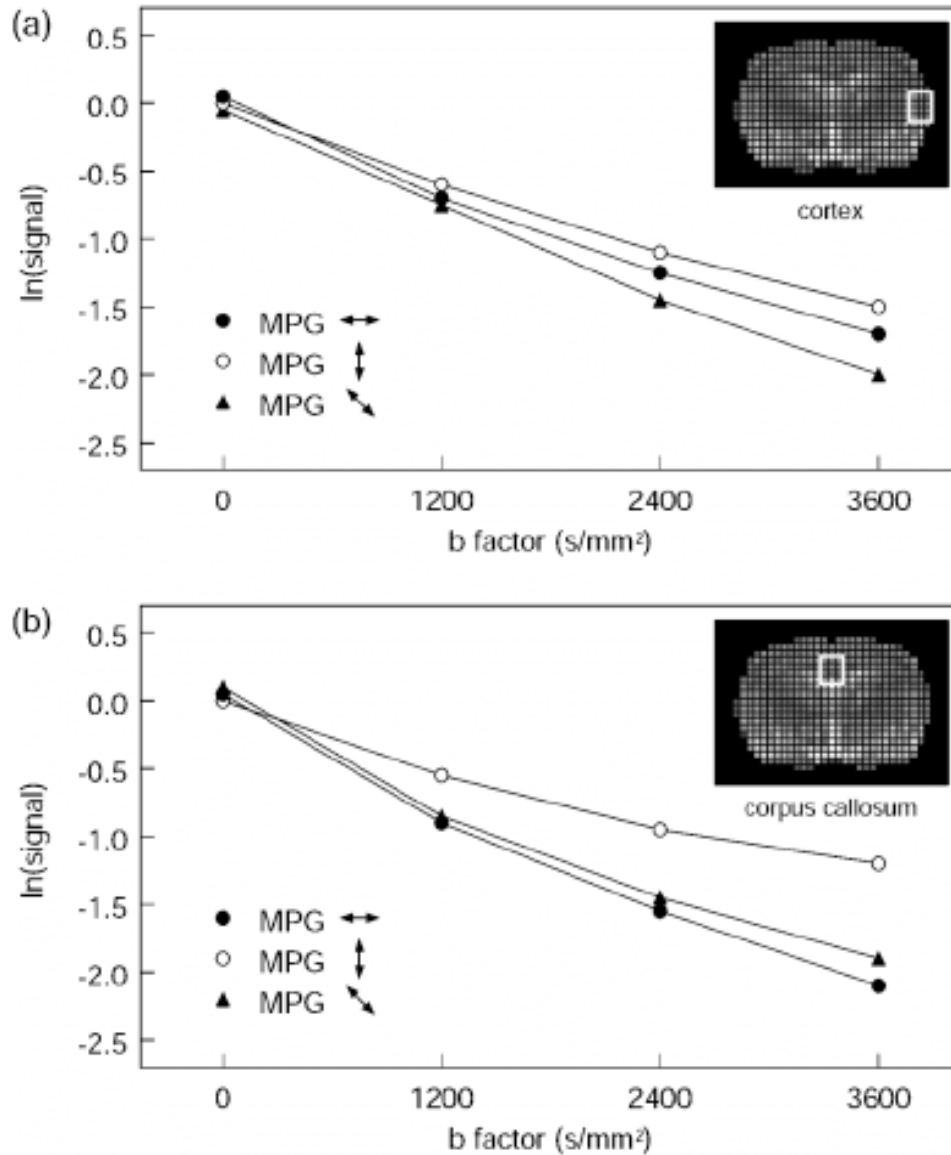


Fig. 7. The Relationships Between The B Factor And The Logarithm Of The Signal Intensity In (A) The Cortex And (B) The Corpus Callosum. The Signals Were Obtained With Mpgs Applied In Three Different Directions. While The Cortex Exhibited Isotropic Signal Attenuations, The Corpus Callosum Exhibited Anisotropic Signal Attenuations [16].

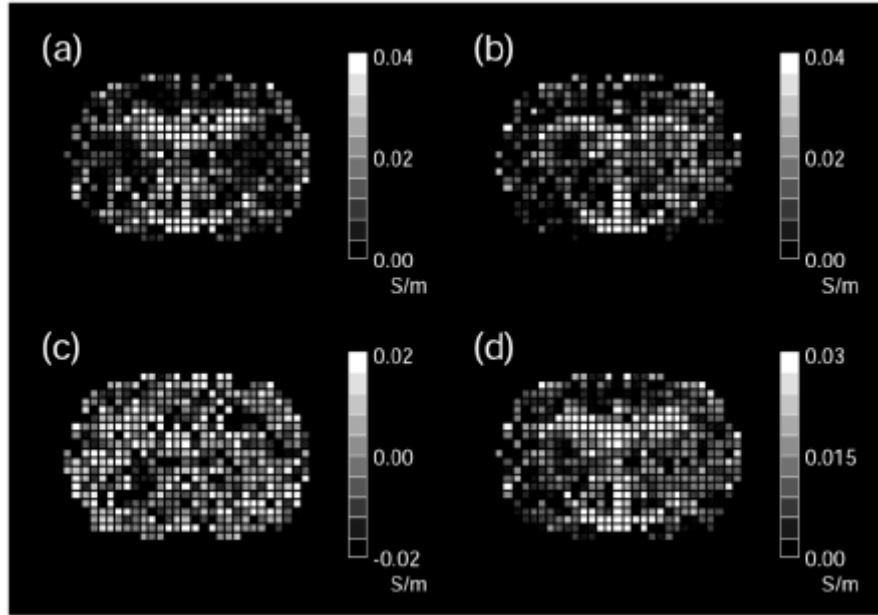


Fig. 8. Distributions of the conductivity tensor components (a) s_{xx} , (b) s_{yy} , (c) s_{xy} , and (d) the mean conductivity [16].

using an equation for the balance of electrostatic force and viscous resistance on an ion, the Stokes-Einstein equation, and the Cole's model of conduction in porous media. Regions-of-interest (ROIs) were located on the cortex and the corpus callosum. The signal attenuation in the corpus callosum exhibited high anisotropy due to alignment of neuronal fibers. The mean conductivities (MCs) in the cortex and the corpus callosum were $(6.14 \pm 0.46) \times 10^{-2} \text{ S m}^{-1}$ and $(7.31 \pm 0.70) \times 10^{-2} \text{ S m}^{-1}$, respectively. The fractional anisotropies (FAs) in the cortex and the corpus callosum were 0.25 ± 0.07 and 0.33 ± 0.03 , respectively. Regions with high conductivity anisotropy were found in the white matter. Measurements of humans were carried out using a 1.5 T MRI system. Images of 5 healthy volunteers were obtained using an echo-planar imaging (EPI) sequence. MPGs were applied with 25 arrayed b factors. The MCs in the cortex, the corpus callosum, and the pyramidal tract were $0.10 \pm 0.03 \text{ S m}^{-1}$, $0.12 \pm 0.02 \text{ S m}^{-1}$, and $0.08 \pm 0.01 \text{ S m}^{-1}$, respectively. The anisotropy indexes (AIs) in the cortex, the corpus callosum, and the pyramidal tract were 0.07 ± 0.03 , 0.60 ± 0.07 , and 0.65 ± 0.05 , respectively. The corpus callosum and the pyramidal tract exhibited high anisotropy in conductivity compared with the cortex. The estimated conductivities were in good agreement with directly measured values of dissected tissues. In conventional methods, conductivity of an organ or a tissue was obtained by measurement of a dissected portion of the organ or the tissue, and conductivity of the organ or the tissue was represented by the measured value. However, this method is not necessarily applicable

to a tissue having inhomogeneous conductivity, for example, white matter in the brain. The proposed method enables measurement of inhomogeneous conductivity of the tissue. The proposed method enables measurement of inhomogeneous conductivity of the tissue.

A distinctive signal inhomogeneity arises in MRI of samples whose dimension is comparable to the wavelength of electromagnetic fields at the resonant frequency. Spatial distributions of magnitude and phase of magnetic resonance signals in cylindrical phantoms were obtained by theoretical calculations and experiments [20,21]. As diameter of the phantom approaches to the wavelength of electromagnetic fields in the phantom, the center of the phantom exhibited high magnitude of signals. An increase in conductivity resulted in a suppression of the signal inhomogeneity due to skin effect. In addition, the increase in conductivity caused a phase delay at the center of the phantom.

Detection of weak magnetic fields induced by neuronal electrical activities using MRI is a potentially effective method for functional imaging of the brain. We performed a numerical analysis of the theoretical limit of sensitivity for detecting weak magnetic fields generated in the human brain [22]. The limit of sensitivity was estimated from the intensities of signal and noise in magnetic resonance images. The signal intensity was calculated with parameters which are commonly used in measurements of the human brain. The noise due to the head was calculated using the finite element method (FEM). The theoretical limit of sensitivity was approximately 10^{-8} T.

[4] CANCER THERAPY

Magnetic force acting on magnetic materials moves the materials along magnetic field gradients. A new method to destruct targeted cells was developed using magnetizable beads and pulsed magnetic force [11,12]. TCC-S leukemic cells were combined with magnetizable beads (diameter = 4.5 ± 0.2 μm , magnetic mass susceptibility = $(16.3 \pm 3) \times 10^{-5}$ m^3/kg). The aggregated cell/bead/antibody complexes were then stimulated by a circular shaped coil which produced a maximum of 2.4 T at the center of the coil. After stimulation, the viability of the cells was measured, and the cells were observed under a scanning electron microscope. The viability of the

aggregated and stimulated cell/bead/antibody complexes was significantly decreased, and the cells were destructed by the penetration of the beads into the cells or rupturing of the cells by the beads, as shown in Fig. 3. We hypothesize that the instantaneous pulsed magnetic forces cause the aggregated beads to forcefully penetrate or rupture the targeted cells. The magnetic force acting on any particular material is proportional to the magnetic field, magnetic field gradient, and the magnetic susceptibility of the material. When the nanoscale particles inside the beads are closely assembled, the magnetic mass susceptibility is sufficiently high to force the attachment of the beads to the cells by the magnetic force. The magnetic force acting on the aggregated beads was strong enough to shift the beads and damage the cells.

We investigated the effects of repetitive magnetic stimulation on tumors and immune functions [13-15]. Magnetic stimulations were applied from a circular coil with the following conditions: peak magnetic field = 0.25 T (at the center of the coil), frequency = 25 pulses/sec, 1000 pulses/sample/day and magnetically induced eddy currents in mice = 0.79 – 1.54 A/m². Tumor growth study showed a significant tumor weight decrease due to the application of magnetic stimulation (54% vs the sham group). An immunological assay was also performed to examine the effects of the magnetic stimulation on immune functions. An *in vivo* study, TNF- α and IL-2 productions in the spleen were measured after exposure of the magnetic stimulation 3 or 7 times. TNF- α production significantly increased in the stimulated group (146 - 164 % vs. the sham group). In an *in vitro* study, isolated spleen cells (lymphocytes) were exposed to the magnetic stimulation (25 pulses/sec, 1000 pulses/sample, and eddy currents: 2.36 – 2.90 A/m²) and a proliferation assay was performed. The proliferation activity of the lymphocytes was up-regulated in the exposed samples. These results indicate that the immune functions might be activated by repetitive magnetic stimulation exposure, resulting in a tumor weight decrease.

[5] CONCLUSION

Biomagnetics and bioimaging are leading medicine and biology into a new horizon through the novel applications. With the increasing integration of medicine and engineering, biomagnetics and bioimaging are further developing into a new science that encompasses a wide range of fields including physics and cognitive science, integrating their diverse cultures to create a new, original discipline.

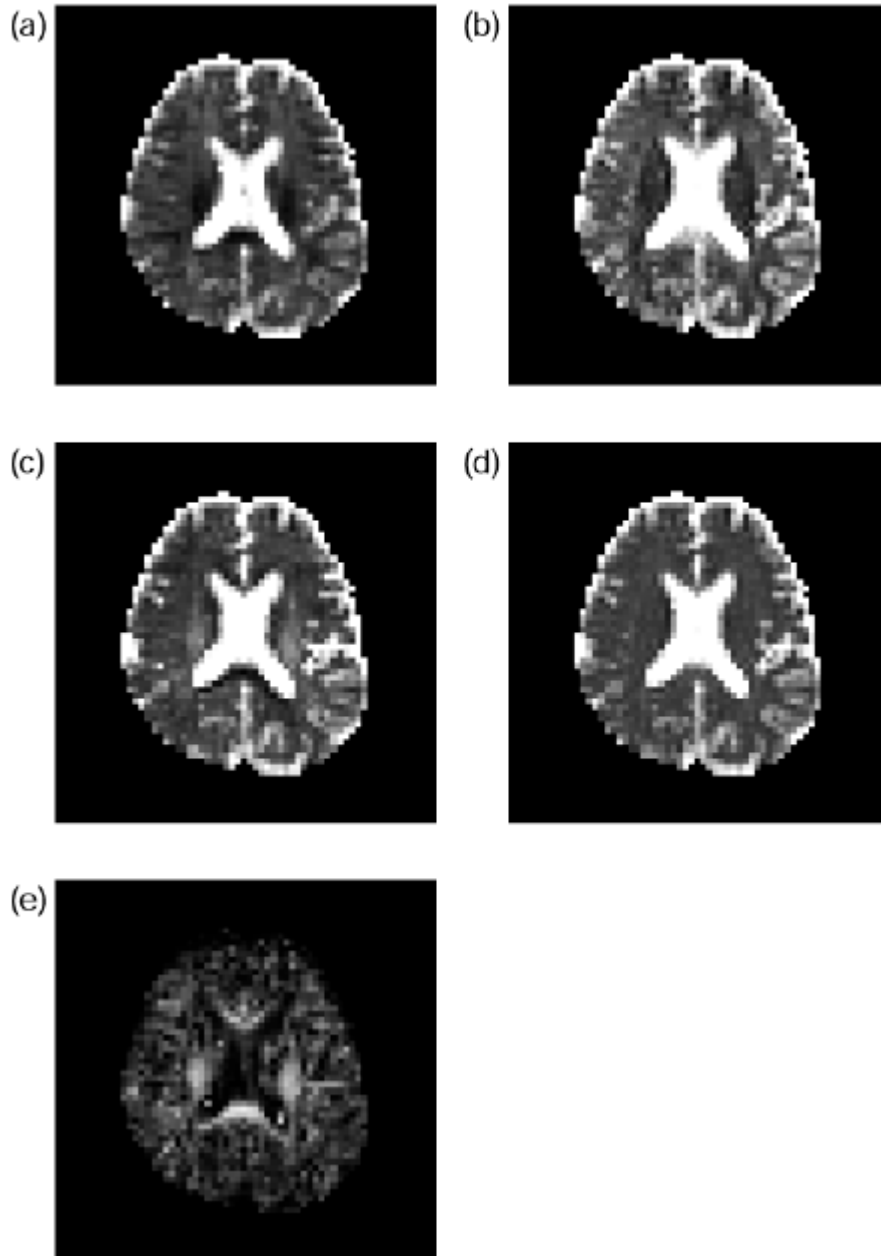


Fig. 9. (A)(B)(C) Images Of The Estimated Conductivities In The Human Brain For The Anterior-Posterior, Right-Left, And Superior-Inferior Directions. (D)(E) Images Of The Mean Conductivity (MC) And The Anisotropy Index (AI) [17].

[6] ACKNOWLEDGEMENT

The author wishes to acknowledge the assistance and support of the COE Steering Committee. This study was supported in part by a Grant-in-Aid for Scientific Research (S) (No. 17100006) from the Japan Society for the Promotion of Science (JSPS).

REFERENCES

- [1] Ueno, S., "Biomagnetic approaches to studying the brain," *IEEE Eng. Med. Biol.*, vol. 18, no. 3, pp. 108-120, May-June 1999.
- [2] Ueno, S., Tashiro, T., and Harada, K., "Localized stimulation of neural tissues in the brain by means of a paired configuration of time-varying magnetic fields," *J. Appl. Phys.*, vol. 64, no. 10, pp. 5862- 5864, November 1988.
- [3] Ueno, S., Matsuda, T., and Fujiki, M., "Functional mapping of the human motor cortex obtained by focal and vectorial magnetic stimulation of the brain," *IEEE Trans. Magn.*, vol. 26, no. 5, pp. 1539- 1544, September 1990.
- [4] Epstein, C. M., Sekino, M., Yamaguchi, K., Kamiya, S., and Ueno, S., "Asymmetries of prefrontal cortex in human episodic memory: Effects of transcranial magnetic stimulation on learning abstract patterns," *Neurosci. Lett.*, vol. 320, No. 1-2, pp. 5-8, March 2002.
- [5] Sekino, M., and Ueno, S., "Comparison of current distributions in electroconvulsive therapy and transcranial magnetic stimulation," *J. Appl. Phys.*, vol. 91, no. 10, pp. 8730-8732, May 2002.
- [6] Sekino, M., and Ueno, S., "FEM-based determination of optimum current distribution in transcranial magnetic stimulation as an alternative to electroconvulsive therapy," *IEEE Trans. Magn.*, vol.40, no. 4, pp. 2167-2169, July 2004.
- [7] Sekino, M., and Ueno, S., "Numerical calculation of eddy currents in transcranial magnetic stimulation for psychiatric treatment," *Neurol. Clin. Neurophysiol.*, vol. 88, p. 1-5, November 2004.
- [8] Ogiue-Ikeda, M., Kawato, S., and Ueno, S., "The effect of repetitive transcranial magnetic stimulation on long-term potentiation in rat hippocampus depends on stimulus intensity," *Brain Res.*, vol. 993, no. 1-2, pp. 222-226, December 2003.
- [9] Ogiue-Ikeda, M., Kawato, S., and Ueno, S., "Acquisition of ischemic tolerance by repetitive transcranial magnetic stimulation in the rat hippocampus," *Brain Res.*, vol. 1037, no. 1-2, pp. 7-11, March 2005.
- [10] Funamizu, H., Ogiue-Ikeda, M., Mukai, H., Kawato, S., and Ueno, S., "Acute repetitive transcranial magnetic stimulation reactivates dopaminergic system in lesion rats," *Neurosci. Lett.*, vol. 383, no. 1-2, pp. 77-81, July 2005.
- [11] Ogiue-Ikeda, M., Sato, Y., and Ueno, S., "A new method to destruct targeted cells using magnetisable beads and pulsed magnetic force," *IEEE Trans. Nanobiosci.*, vol. 2, no. 4, pp. 262-265, December 2003.
- [12] Ogiue-Ikeda, M., Sato, Y., and Ueno, S., "Destruction of targeted cancer cells using magnetizable beads and pulsed magnetic forces," *IEEE Trans. Magn.*, vol. 40, no. 4, pp. 3018-3020, July 2004.
- [13] Yamaguchi, S., Ogiue-Ikeda, M., Sekino, M., and Ueno, S., "The effect of repetitive magnetic stimulation on the tumor development," *IEEE Trans. Magn.*, vol. 40, no. 4, pp. 3021-3023, July 2004.
- [14] Yamaguchi, S., Ogiue-Ikeda, M., Sekino, M., and Ueno, S., "Effects of magnetic stimulation on tumors and immune functions," *IEEE Trans. Magn.*, (in press).

- [15] Yamaguchi, S., Ogiue-Ikeda, M., Sekino, M., and Ueno, S., "Effects of pulsed magnetic stimulation on tumor development and immune functions in mice," *Bioelectromagnetics*, (in press).
- [16] Sekino, M., Yamaguchi, K., Iriguchi, N., and Ueno, S., "Conductivity tensor imaging of the brain using diffusion-weighted magnetic resonance imaging," *J. Appl. Phys.*, vol. 93, no. 10, pp. 6730-6732, May 2003.
- [17] Sekino, M., Inoue, Y., and Ueno, S., "Magnetic resonance imaging of mean values and anisotropy of electrical conductivity in the human brain," *Neurol. Clin. Neurophysiol.*, vol. 55, pp. 1-5, November 2004.
- [18] Sekino, M., Matsumoto, T., Yamaguchi, K., Iriguchi, N., and Ueno, S., "A method for NMR imaging of a magnetic field generated by electric current," *IEEE Trans. Magn.*, vol. 40, no. 4, pp. 2188-2190, July 2004.
- [19] Yamaguchi, K., Sekino, M., Iriguchi, N., and Ueno, S., "Current distribution image of the rat brain using diffusion weighted magnetic resonance imaging," *J. Appl. Phys.*, vol. 93, pp. 6739-6741, May 2003.
- [20] Sekino, M., Mihara, H., Iriguchi, N., and Ueno, S., "Dielectric resonance in magnetic resonance imaging: Signal inhomogeneities in samples of high permittivity," *J. Appl. Phys.*, vol. 97, no. 10, pp. 10R303, May 2005.
- [21] Mihara, H., Iriguchi, N., and Ueno, S., "Imaging of the dielectric resonance effect in high field magnetic resonance imaging," *J. Appl. Phys.*, vol. 97, no. 10, pp. 10R305, May 2005.
- [22] Hatada, T., Sekino, M., and Ueno, S., "Detection of weak magnetic fields induced by electrical currents with MRI: Theoretical and practical limits of sensitivity," *Magn. Reson. Med. Sci.*, vol. 3, no. 4, pp. 159-163, March 2004.
- [23] Hatada, T., Sekino, M., and Ueno, S., "FEM-based calculation of the theoretical limit of sensitivity for detecting weak magnetic fields in the human brain using magnetic resonance imaging," *J. Appl. Phys.*, vol. 97, no. 10, pp. 10E109, May 2005.